Pectin–Tin(IV) molybdosilicate: An ecofriendly cationic exchanger and its potential for sorption of heavy metals from aqueous solutions

Nimisha K. V *, Aparna Mohan, Janardanan. C

Post Graduate and Research Department of Chemistry, Sree Narayana College, Kannur, Kerala 670007, India

Abstract

A novel composite cation exchanger of biopolymer Pectin and Tin(IV) molybdosilicate heteropoly acid salt were prepared by co-precipitation technique. Physico-chemical characterization of Pectin–Tin(IV) molybdosilicate was performed using instrumental techniques such as FTIR, TG, XRD and SEM–EDS. Studies were carried out to investigate ion exchange capacity. pH titration carried out shows cationic nature and polyfunctionality of the exchanger. Distribution coefficients of various metal ions were done to explore the ion exchange behavior of cation exchanger. Distribution studies show that the material is highly selective for toxic heavy metal ions such as Cd^{2+}, Cu^{2+}, Al^{3+} etc. To investigate the environmental applicability of the exchanger some analytically important binary separations and selective separation of metal ions from industrial effluents were achieved. Kinetic and isotherm parameters were evaluated to predict the mechanism of sorption of heavy metal ions. Mass transfer analysis shows that internal particle diffusion and some degree of boundary layer control the sorption process.

1. Introduction

The increasing industrial use of heavy metals over the past decades has lead to a corresponding incremental release of metals in the environment [1]. These metal ions may be introduced into natural waters from industries such as metal plating facilities, mining operations, fertilizer industries, tanneries, batteries, paper industries, pesticides etc. and these materials in turn enter the human body through inhalation and ingestion of food and drinking water [2]. Insufficiently or partially treated industrial effluents induce unacceptable sanitary risk and environmental hazards in all natural compartments especially in water bodies. Most toxic metal ions even in low concentration have got great impact on socioeconomic activities of humans and animals due to their biopersistence in the organism and ecosystem [3]. The exposure of these hazardous materials in high concentration leads to chemical pneumonitis, pulmonary edema, neuropathy, abdominal pains, etc.

Various chemical and physical methodologies such as adsorption [4], coagulation [5], reverse osmosis [6], photocatalysis [7], ion exchange [8] etc. were employed as well as known technology for the treatment of waters rich in metallic pollutants. Among these sorption by ion exchange materials has attracted interest due to their wide applicability, more selectivity and cost effectiveness in waste water treatment technologies [9]. A number of organic and inorganic materials such as humins, humic acids, clay and zeolite were available in nature which exhibit ion exchange properties. Plenty of exchangers that mimic properties of natural exchangers were synthesized in lab by many researchers. These are organic polymeric resins, oxides and hydrous oxides, acid salts of polyvalent metals, heteropoly acids and aluminosilicates [10–13].

The conversion of organic and inorganic ion-exchange materials into hybrid ion exchangers is the latest development in this discipline and has got great attention. Composite can combine the properties of both components and offer special properties through modification of its structure [14]. Besides other advantages, composite ion exchange materials are more stable at high temperature and radiation fields [15].

In recent years, biocomposites which incorporate the advantageous properties of both biopolymers and inorganic materials

---

* Corresponding author. Post Graduate and Research Department of Chemistry, Sree Narayana College, Kannur, Kerala 670007, India. Tel.: +91 9496971255.

E-mail address: nimishavijil89@gmail.com (N.K. V).

have received an increasing attention as ion exchange adsorbents for removal of various pollutants due to their structural and functional properties [16]. Bio polymers such as cellulose acetate, pectin, chitosan etc. have been used as organic polymeric part for the fabrication of biocomposites [17–19]. This could bring a large range of improved properties like stiffness, permeability, crystallinity and thermal stability, high exchange capacity and selectivity with preservation of the material biodegradability, without showing eco-toxicity results in the formation of green composite. Biopolymer incorporation provides greater mechanical strength and stability and also presence of various hydroxyl and carboxyl groups in the polymeric matrix increases the number of active surface sites which enhances its ion exchange properties. Thus it enhances the selective metal sorption capacity of the exchangers. Pectin is important naturally occurring biopolymer of plant origin. Use of pectin as organic backbone is gaining attention because of its inexpensive, easy availability and its macro molecular nature and can easily bind with inorganic substances via molecular interactions [20,21].

The present work deals with synthesis and properties of novel biopolymer based composite exchanger Pectin–Tin(IV) molybdosilicate. Composite formation was confirmed by FTIR, TG, XRD, SEM and EDX techniques. Also, analyses of applicability of the material for the removal of metal ions Cd^{2+} and Cu^{2+} from industrial waste water were investigated. In order to understand the rate controlling mechanism and feasibility of adsorption of ion exchanger kinetic and thermodynamic parameters for the sorption of Cu^{2+} were evaluated.

2. Experimental

2.1. Reagents and methods

All the chemicals and reagents used were of analytical grade and measured without further purification. The main reagents used for the synthesis of the composite material were Stannic chloride (LobaChemie), Ammonium molybdate (E.Merck), Sodium silicate (LobaChemie), Pectin (Lobachemie). Double distilled water was used for preparing the solutions of different concentrations.

2.2. Instrumentation

A glass column was used for column process. ELICO LI613 pH meter was used for pH measurements. FT-IR Spectrometer model Thermo-Nicolet Avtar 370 (Japan) were taken by KBr disk method at room temperature for IR studies, X-ray Diffractometer Bruker AXS D8 (Japan) Advance for X-ray diffraction studies with Cu Kα radiations, TG Perkin Elmer Diamond TG/DTA (USA) Analysis System for thermogravimetric/derivative thermogravimetric analysis and were used at a rate of 10 °C in nitrogen atmosphere. UV–Visible Spectrophotometer model JASCO V660 (Japan) was used for spectrophotometric measurements. Jeol Model JSM-6390LV for SEM analysis, Jeol Model-Jed-2300 (USA) was used for Energy Dispersive Spectrometric analysis. Magnetic stirrer (Remi Equipments) was used for stirring purposes.

2.3. Synthesis

2.3.1. Synthesis of Tin(IV) molybdosilicate (SnMoSi) exchanger

Inorganic gels of SnMoSi were prepared by mixing boiling aqueous solutions of ammonium molybdate and sodium silicate upon vigorous stirring. pH was adjusted to acidic by adding 1.0 M HNO$_3$ drop wise, the gelatinous precipitate locally formed disappears upon stirring. After boiling for a few minutes, the clear solution was precipitated by addition of an aqueous solution of Stannic chloride. A white gelatinous precipitate was formed. Constant stirring was maintained using a magnetic stirrer at room temperature (25 ± 2 °C) for 3 h. The gel obtained was left for 24 h at room temperature for digestion. The excess reagents were removed by filtration. After washing with demineralized water (DMW) the precipitate obtained was dried convert into H$^+$ form by immersing in 1.0 M HNO$_3$ solution with intermittent replacement of acid at an interval of 2 h.

2.3.2. Synthesis of pectin gels

Pectin gels were prepared by dissolving varying amount (1–3 g) of pectin powders in DMW with vigorous stirring.

2.3.3. Synthesis of Pectin–Tin (IV) molybdosilicate

Pectin–Tin(IV) molybdosilicate was prepared by simple mixing of pectin gels with inorganic precipitate of Tin(IV) molybdosilicate. The yellow colored gel was kept for 24 h at room temperature (25 ± 2 °C) for digestion. The supernatant liquid was decanted and the gel was filtered. The excess acid was removed by washing with DMW and the material was dried in an air oven at 30 °C. The dried products were immersed in DMW to obtain small granules. They were converted to H$^+$ form by treating with 1.0 M HNO$_3$ for 24 h with occasional shaking, intermittently replacing the supernatant liquid with fresh acid. The excess acid was removed after several washings with DMW and then dried at 30 °C. The particles size of the range (125 µm) was obtained by sieving and was kept in desiccators.

2.4. Physico chemical characterization

2.4.1. Ion exchange capacity

The IEC of the materials were determined by the column process; 1.0 g of the exchangers (H$^+$ form) was filled in a glass column of 1.1 cm diameter. The H$^+$ ions were eluted by adding 100 mL of 1.0 M sodium chloride solution. The effluent was collected at the bottom and titrated against standard sodium hydroxide solution. The ion exchange capacity in meq/g was calculated using the formula (eqn. (1)):

$$IEC = \frac{av}{w} \tag{1}$$

where 'a' is the molarity, 'v' is the volume of alkali used during titration and 'w' is the weight of the exchanger taken [22].

2.4.2. Chemical stability

The chemical stability of the exchangers was assessed in mineral acids like HCl, HNO$_3$ and H$_2$SO$_4$, bases like NaOH and KOH and organic solvents like acetic acid, acetone, ethanol and

diethyl ether. For this 500 mg of the exchanger was separately in 50 mL of different solvents at room temperature for 24 h. The changes in color and weight were noted.

2.4.3. pH titration curve

Topp and Pepper method [23] was used for pH titration studies of exchangers using NaOH/NaCl and KOH/KCl systems. For this 500 mg of exchanger was equilibrated with different amounts of metal chloride and metal hydroxide solutions. pH of each solution was measured after attainment of equilibrium and was plotted against milliequivalents of OH⁻ ions added.

2.4.4. Partition coefficient (sorption) studies

Sorption studies were carried out for various heavy metal ions in demineralized water (DMW) by batch method. The distributions of metal ions before and after equilibrium were determined volumetrically using EDTA as the titrant. The distribution coefficient (K_d) values were calculated using the formula (eqn. (2))

$$K_d = \frac{(I-F)}{F} \times \frac{V}{W} \tag{2}$$

where 'I' is the initial volume of EDTA used, 'F' is the final volume of EDTA used, 'v' is the volume of the metal ion solution and 'w' is the weight of the exchanger used .

2.5. Analytical applications

2.5.1. Quantitative separation of metal ions in binary synthetic mixtures

Quantitative binary separation of some metal ions of analytical utility was attained on the column of Pc–SnMoSi exchanger. The column on which the separations were to be carried out was filled uniformly with the Pc–SnMoSi composite exchanger in the H⁺ form. Initially distilled water was added to pack the granules so that no air bubbles get stuck. Binary mixture of the metal ions to be separated was poured on to the column and allow to flow at a rate of 0.3–0.5 mL min⁻¹. The above process was repeated for to ensure maximum sorption of metal ions on the exchanger. Individual metal ions were eluted using appropriate eluting reagents. The flow rate of the eluent was maintained (0.3–0.5 mL·min⁻¹) throughout the process of elution. The effluent was collected at the bottom and was titrated against the standard solution of di-sodium salt of EDTA.

2.5.2. Quantitative separation of metal ions from industrial waste water

Different samples of waste water were collected from the outlet glassy metal plating industry, Calicut and Phosphate Fertilizer industry, Cochin. The effluent samples were filtered using filter paper first to remove suspended particle and then neutralized. The solution was decolorized using normal charcoal. The effluent samples thus obtained were characterized by standard methods to detect heavy metal present in it. Qualitative analysis of filtered effluents helps to find out the metal present in it, and shows that metal plating industry waste water contains

Cu (II) and that of fertilizer plant contains Cd (II) ions. The granular ion exchanger Pc–SnMoSi having greater selectivity toward heavy metals Cu(II) and Cd(II) were packed in a column, 100 mL of the effluents were passed through the separate column of the composite exchanger. The flow rate was maintained at 0.3–0.5 mL/min. Finally the ions were separated using suitable eluents and determined quantitatively.

2.6. Kinetic studies

Composite cation exchange particles of mean radii ~125 μm (50–70 mesh) in H⁺ form were used to evaluate various kinetic parameters. The rate of exchange was determined by limited batch technique as follows.

A total of 20 mL fractions of the 0.02 M metal ion solutions (Cu (II)) were shaken with 200 mg of the cation exchanger in H⁺ form in several conical flasks at desired temperatures (30, 40, 50 and 60 (±0.5 °C)) for different time intervals (5, 10, 20, 30, 40 m). The supernatant liquid was removed immediately and determinations were made as usual by ethylene diammine tetra acetic acid, di-sodium salt (EDTA) titrations. Each set was repeated three times and the mean values were taken for calculation.

2.7. Desorption and regeneration

In order to check the reusability of the exchanger desorption and regeneration experiments were conducted as follows.

Metal ion loaded exchanger was separated from the batch adsorption system and by centrifugation and gently washed with distilled water to remove unadsorbed metal ions. Cu(II) loaded exchanger was then treated with 1.5 M HNO₃ and Cd(II) loaded exchanger was with 1.0 M HCl for 2 h. The concentrations of metal ions were determined by EDTA titrations of the solution and amount of desorbed ions was computed using initial and final concentrations of metal ions. The regenerated spent adsorbent was reused and the loading and regeneration were repeated 4 times.

3. Results and discussions

3.1. Physico chemical properties

Tin(IV) molybdosilicate samples of different compositions were synthesized and ion exchange capacity was determined (Table 1). Among these the sample, SnMoSi-2, having maximum IEC (0.97 meq/g) was selected and was incorporated into the biopolymeric matrix of pectin by varying its mixing volume percentage. Analysis of IEC of composite material reveals that Pc–SnMoSi-3 shows higher IEC (1.82 meq/g) among the entire composite and also than its inorganic counterpart. This may be due to availability of additional freely movable H⁺ ions and H₂O molecules situated in the cavities of the polymeric matrix after composite formation. Therefore sample with this composition was selected for further studies.

Pc–SnMoSi is most stable in acid medium, especially with lower molarity. And also stable in 0.1 M basic media, 1.0 M salt solutions and organic solvents like ethanol, acetone, carbon tetrachloride etc. Pc–SnMoSi was found to be quite stable in different concentrations of mineral acids such as 10.0 M HNO₃,

Table 1
Condition for the preparations of various samples of Pc–SnMoSi composite cation exchange material.

Samples	Mixing volume ratio				pH	Appearance	Na$^+$ IEC(meq/g)
	A	B	C	D			
SnMoSi-1	1	1	1	–	1	White granular	0.91
SnMoSi -2	1	2	1	–	1	White granular	0.97
SnMoSi -3	2	1	1	–	0.5	White granular	0.43
SnMoSi -4	1	1	2	–	1	White granular	0.68
SnMoSi -5	1	2	2	–	1	White granular	0.54
SnMoSi -6	2	2	1	–	0.5	White granular	0.81
Pc–SnMoSi -1	1	2	1	1	1	Fleshy granular	1.22
Pc–SnMoSi -2	1	2	1	2	1	Fleshy granular	0.99
Pc–SnMoSi -3	1	2	1	3	1	Fleshy granular	1.82

A, 0.1M $SnCl_4.5H_2O$ in DMW.
B, 0.1M $Na_2MO_4.2H_2O$ in DMW.
C, 0.1M $Na_2SiO_3.9H_2O$ in DMW.
D, % of pectin in DMW.

5.0 M H_2SO_4 and 12.0 M HCl, 0.05 M solutions of bases and organic solvents like ethanol, acetone, CCl_4, DMSO, DMF etc.

pH titration curve gives information about functionality behavior and nature of ionogenic group of the exchanger. Fig. 1(a) and (b) shows pH titration curves of SnMoSi and Pc–SnMoSi respectively have drawn for NaOH/NaCl and KOH/KCl systems. Both of them show more than one inflection points as indicated by sudden change in pH, inferring polyfunctional nature of both composite and its inorganic counterpart. Both appear to be strong cation exchangers as indicated by a low pH (~2–3) of the solution in neutral media, i.e., before the addition of NaOH to NaCl solution. Composite was found to be highly acidic as indicated by very low pH values compared to inorganic counterpart. The ion exchange capacity of the strong acidic groups of the composite ion exchanger determined from graph is 1.67 meq/g and is in agreement with that obtained from the column process.

FTIR spectrum of SnMoSi and Pc–SnMoSi was shown in Fig. 2(a) and (b). FTIR spectrum of SnMoSi (Fig. 2(a)) shows a broad band at 3385 cm^{-1} and a sharp peak at 1630 cm^{-1}, justifying the presence of —OH stretching and bending modes. A sharp peak at 1107 cm^{-1} is attributed to silicate ion and number of peaks observed at 560–800 cm^{-1} was due to metal oxygen bond and the band at 940 cm^{-1} shows the presence of molybdate ion. The sharp band 1380 cm^{-1} attributed to the presence of δ (Si—OH) indicates the presence of structural hydroxyl protons in SnMoSi [24]. The peak values of FTIR spectra (Fig. 2(b)) of Pc–SnMoSi show a broad band centered at 3400 cm^{-1} indicating the characteristics of O—H stretching vibrations. The peak present at 1097 and 1143 cm^{-1} is assigned to C=O and C=C double bond of pectin. The band observed at 1740 was due to the presence of C=O stretching of ester. The peaks at 1377 cm^{-1} may be due to stretching bands of free COO$^-$ group in pectin [25]. Also peaks associated with oxides and metal hydroxides were also present below 600 cm^{-1} region with slight shift in peak position and intensities. This clearly indicates the composite formation by the incorporation of SnMoSi and pectin.
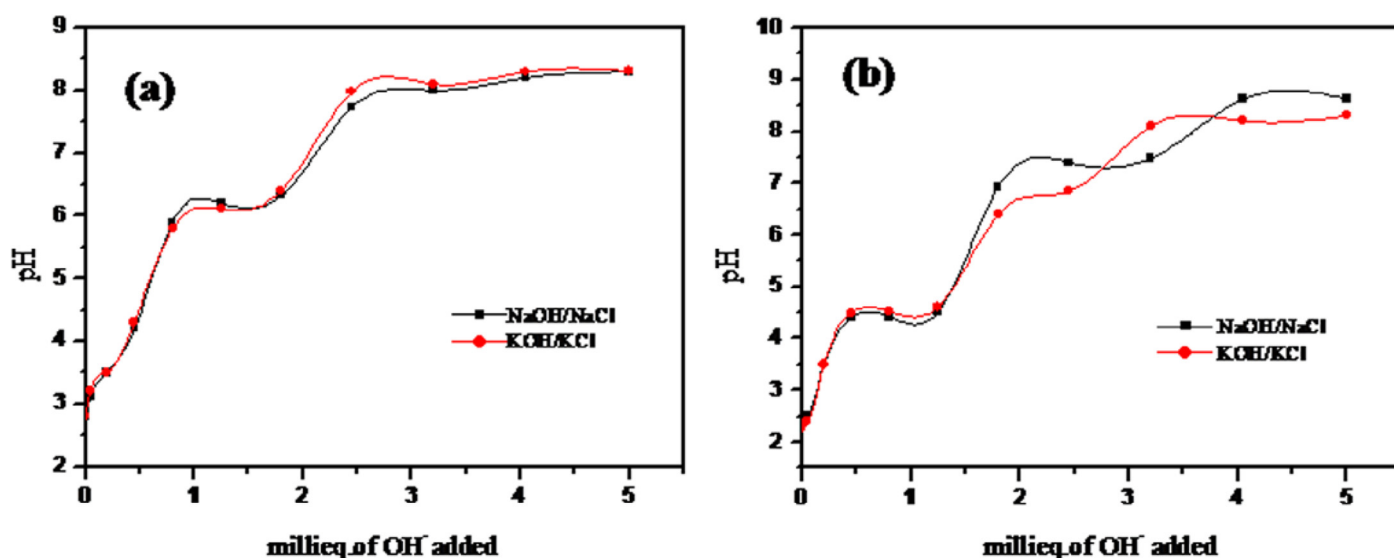
TG-DTG scans recorded for SnMoSi and Pc–SnMoSi are shown in Fig. 3(a) and (b). It is clear from figure that thermal decomposition of SnMoSi occurs mainly in two stages. In the first stage of decomposition (50–150 °C) 18% weight loss observed is due to dehydration, whereas a continuous loss of around 32% was observed during second stage, which is ascribed to decomposition and conversion of SnMoSi to oxide form. Pc–SnMoSi undergoes degradation mainly in three stages. Initial weight loss of 25% in the 50–160 °C is due to moisture loss from surface and internal layer of the material. The second stage resulting in 40% loss at 200–700 °C implies the degradation of biopolymer networks. Third stage of decomposition starts above 700 °C due to conversion of the material into its oxide form and up to 800 °C heating temperature, 56% of the material was retained.

The XRD patterns provide significant information in relation to the nature and size of the sample. The X-ray diffraction patterns of inorganic precipitate and its pectin composite were

Fig. 1. pH titration curve of (a) SnMoSi and (b) Pc–SnMoSi.
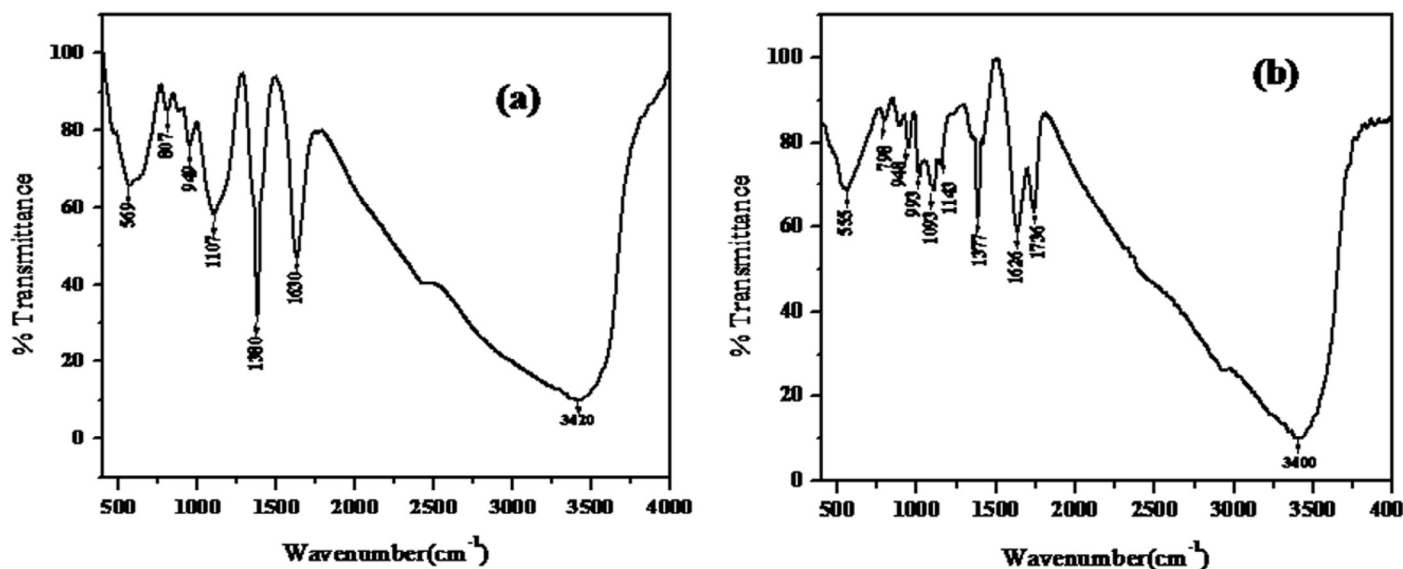
Fig. 2. FTIR of (a) SnMoSi and (b) Pc–SnMoSi.

shown in Fig. 4(a) and (b). XRD pattern of both SnMoSi composite and Pc–SnMoSi sample shows semicrystalline nature as indicated by low intensity peaks.

Fig. 5(a) and (b) shows the SEM pictures of SnMoSi and Pc–SnMoSi respectively. The significantly different morphologies were obtained by the incorporation of pectin on to the SnMoSi matrix. Micrograph of SnMoSi shows the undefined aggregated morphology and Pc–SnMoSi shows fluffy smoothened appearance with some pores. Porous nature increases rate of ion exchange capacity, and increases the surface area and catalytic activity of composite.

Compositional analyses of SnMoSi and Pc–SnMoSi samples were carried out by EDX and histograms are shown in Fig. 6(a) and (b). The presence of all elements i.e., Sn, Mo, Si and O in Fig. 6(a) shows the formation of SnMoSi without any impurity. In the EDX pattern of Pc–SnMoSi in addition to peaks of Sn, Mo, Si and O elements peak corresponding to C and O of groups of pectin also present which confirms the composite formation.

In TGA data and IR studies, the tentative mixed oxide formulas suggested for SnMoSi and Pc–SnMoSi were $[(SnO_2).(H_2MoO_4).(SiO_2)].nH_2O$ and $[(SnO_2)_5.(H_2MoO_4).(SiO_2)_3-(C_7H_{10}O_7)_2-.nH_2O$. The number of water molecules (n) was determined using Alberti–Torroca formula (eqn. (3)),

$$18n = \frac{x(M+18n)}{100} \tag{3}$$

where x is the percentage of water content and (M+18n) is the molar mass of the material. The numbers of water molecules calculated were 4 and 6 for SnMoSi and Pc–SnMoSi, which include that due to condensation of structural hydroxyl groups.

To explore the potential of composite exchangers for the separation of metal ions detailed analysis of K_d values in aqueous media (DMW) and different electrolyte media is necessary. K_d value calculated for DMW and different concentrations of electrolyte solution on synthesized composite ion exchanger Pc–SnMoSi (Table 2) shows that it is highly selective for Cu^{2+}
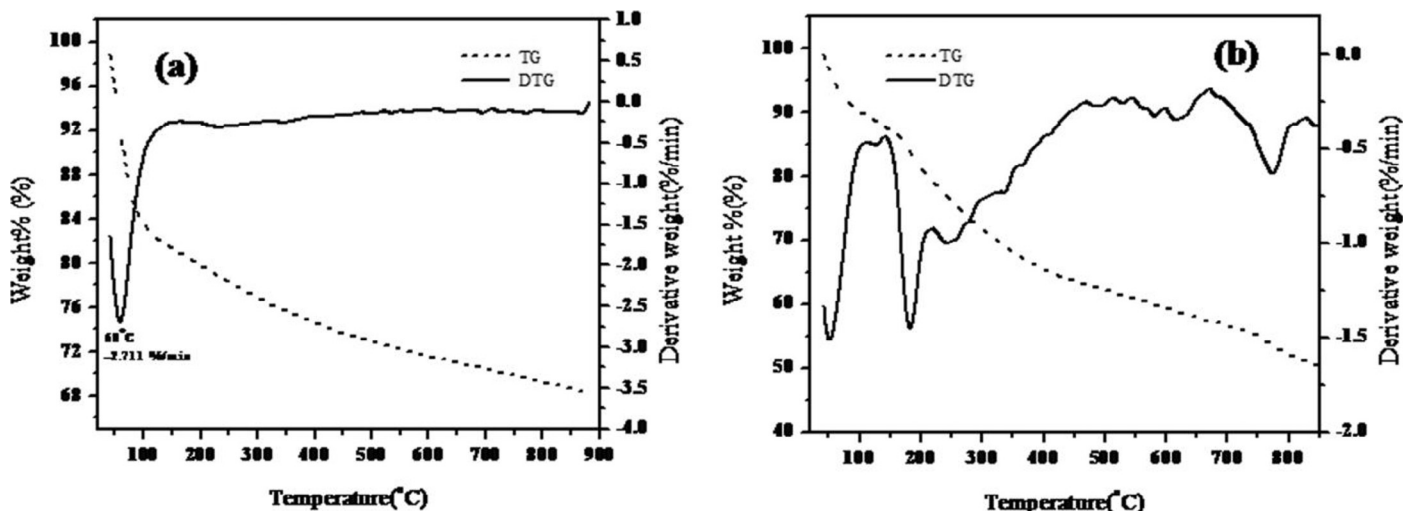
Fig. 3. TG-DTG of (a) SnMoSi and (b) Pc–SnMoSi.
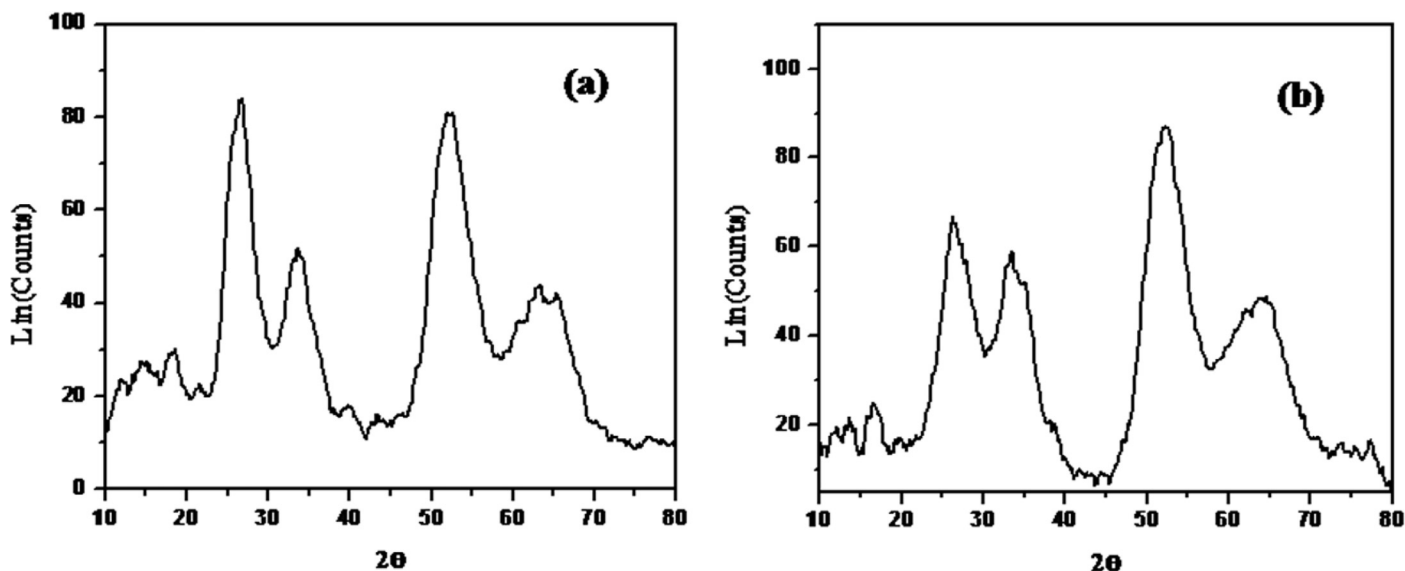
Fig. 4. XRD of (a) SnMoSi and (b) Pc–SnMoSi.

and Cd^{2+} ions and selectivity order is $Cd^{2+} > Cu^{2+} > Al^{3+} > Mn^{2+} > Hg^{2+} > Pb^{2+} > Zn^{2+} > Ca^{2+} > Mg^{2+} > Co^{2+} > Ni^{2+} > Bi^{3+} > Th^{4+}$. Also, with increasing concentration of electrolyte K_d value decreases. The low K_d values for all metal ions in high electrolyte concentration are due to the presence of high concentration of positive ions which reverses the process of ion exchange and the process of regeneration predominates over the process of removal. Also, with increase in the electrolyte concentration, deprotonation on the surface of the exchanger decreases and this decreases the electrostatic interaction with each metal ion. These studies give suggestions regarding the selection of suitable eluents for the separation of binary metal ion mixtures. Hence, the metal ions can be removed in the solvent systems where they are more significantly selective.

3.2. Analytical applications

3.2.1. Quantitative separation of metal ions in binary synthetic mixtures

Based on the K_d values binary separations of some analytically important metal ions were carried out on the column of exchangers. The separations such as Cu^{2+}–Bi^{3+}, Cd^{2+}–Bi^{3+}, Cu^{2+}–Ni^{2+} and Cd^{2+}–Th^{4+}, Al^{3+}–Bi^{3+} were achieved on the composite exchanger Pc–SnMoSi. The separation is based on sequential elution of metal ions through the column using different eluting agents such as different concentrations of NH_4NO_3 and HNO_3. The weakly retained metal ions get eluted first, followed by stronger one using suitable eluents. The order of elution and the eluents used for the separations are shown in Table 3. The separations are quite sharp and recovery is found to be quantitative and reproducible. The recovery range is from 94 to 98% with a variation of $(\pm)1\%$ for repetitive determinations.

3.2.2. Quantitative separation of metal ions from industrial waste water

The extremely high sorption behavior for Cu(II) and Cd(II) metal ions makes the cation exchanger Pc–SnMoSi useful for their removal from waste effluents. Qualitative analysis of waste effluents collected from glassy metal plating industry effluents, Calicut shows presence of Cu(II) ions and that of phosphate fertilizer industry effluents, Cochin contains Cd(II) ions. Two different samples collected from each industry were analyzed
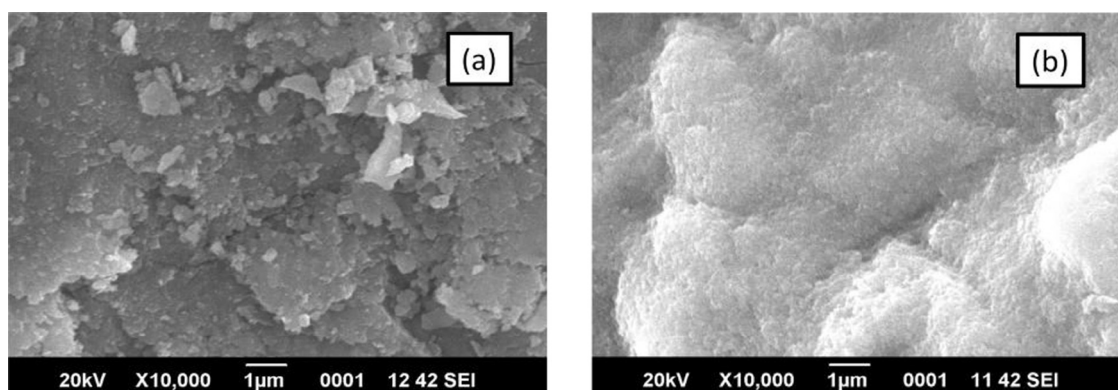
Fig. 5. SEM images of (a) SnMoSi and (b) Pc–SnMoSi.
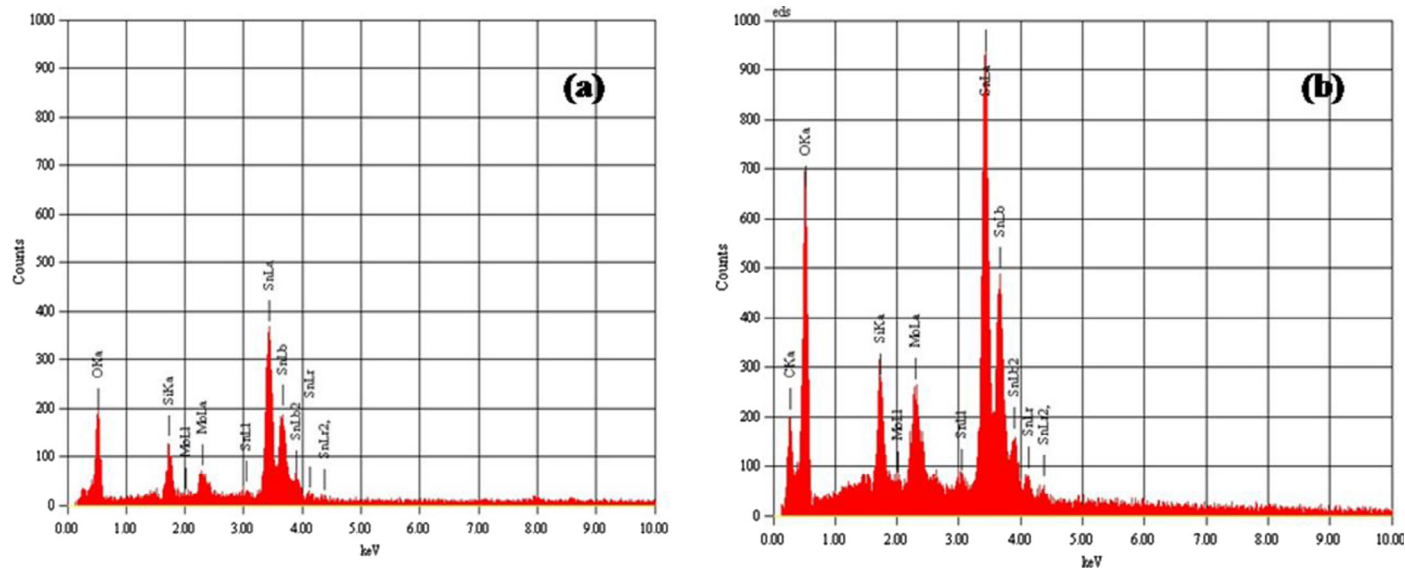
Fig. 6. EDX of (a) SnMoSi and (b) Pc–SnMoSi.

for metal ion recovery using Pc–SnMoSi column. The eluents used were 0.01 M NH_4NO_3 for Cd(II) ions and 0.1 M NH_4NO_3 for Cu(II) ions. Cd(II) sorbed exchanger can be regenerated converting it in H^+ form using 1.0 M HNO_3 and Cu(II) exchanger can be regenerated using 0.5 M HNO_3. Analysis results summarized in Table 4 show that 100 mL of the fertilizer industry effluent contains 1.38–1.40 mg Cd (II) ions and metal plating industry effluents contain 1.65–1.78 mg of Cu (II) ions. Elution curve drawn for the recovery of metal ions was presented in Fig. 7. Elution curve clearly shows that most of the H^+ ions are eluted out in the first 100 mL of eluent using 500 mg of the exchanger. All elution curve shows a maxima around 30–50 mL of eluent. This may be due to adequate availability of exchanging H^+ ions and easy penetration of metal ions into the pores of the exchanger. Elution studies show that column operation efficiency is quite satisfactory. Thus Pc–SnMoSi composite

exchanger offers a cost-effective and technically viable option for treatment of cadmium and copper contaminated wastewater.

3.3. Sorption kinetics and mass transfer

Controlling mechanism and rate of adsorption process were investigated using pseudo-first-order model of Lagergren and pseudo-second-order model of Ho and McKay using linear regression analysis [26] and were formulated as

Table 3
Binary separation of metal ions on Pc–SnMoSi column.

Separations achieved	Eluent	Metal ion (mg)		% Efficiency
		Loaded	Eluted	
Cu^{2+}	0.05 M NH_4NO_3	1.54	1.51	98.05
Bi^{3+}	1.0 M HNO_3 + 0.1 M NH_4NO_3	5.17	5.02	97.09
Cd^{2+}	0.01 M NH_4NO_3	2.69	2.59	96.24
Bi^{3+}	1.0 M HNO_3 + 0.1 M NH_4NO_3	5.18	4.99	96.33
Cu^{2+}	0.05 M NH_4NO_3	1.53	1.48	96.73
Ni^{2+}	0.2 M HNO_3 + 0.1 M NH_4NO_3	1.48	1.45	97.97
Cd^{2+}	0.01 M NH_4NO_3	2.68	2.53	94.42
Th^{4+}	0.05 M HNO_3 + 0.1 M NH_4NO_3	5.80	5.71	98.41
Al^{3+}	0.5 M NH_4NO_3	1.68	1.65	98.21
Bi^{3+}	1.0 M HNO_3 + 0.1 M NH_4NO_3	5.18	4.92	94.96

Table 2
Distribution coefficients in water and other electrolytes.

Cations	Distribution coefficients (K_d)						
	DMW	HNO_3			NH_4NO_3		
		0.001 M	0.01 M	0.1 M	0.001 M	0.01 M	0.1 M
Bi^{3+}	61.3	57.6	50.8	42	59.2	53.5	47.6
Th^{4+}	21.6	15.6	3.0	NS	17.7	9.4	3.1
Ni^{2+}	97.7	84.2	76.3	61.2	87.4	80.6	77.0
Pb^{2+}	215.7	195.4	176.2	134.3	207.0	184.7	162.9
Co^{2+}	169.4	138.7	111.5	94.0	158.1	146.6	120.6
Zn^{2+}	213.1	186.4	147.6	118.2	192.7	153.5	137.8
Mg^{2+}	175.8	137.7	98.2	86.4	158.4	101.6	97.9
Cu^{2+}	441.9	407.0	395.5	374.2	430.3	417.6	401.0
Mn^{2+}	352.1	317.5	295.0	276.3	338.4	317.8	304.6
Cd^{2+}	537.5	468.8	407.3	368.5	487.5	418.2	384.4
Al^{3+}	375.0	336.8	274.7	204.5	358.5	281.2	210.1
Hg^{2+}	300.5	244.3	203.8	187.7	252.6	218.9	191.7
Ca^{2+}	182.5	108.7	95.5	84.0	117.3	101.0	92.8

NS, no sorption.

Table 4
Quantitative removal of Cd^{2+} from fertilizer effluents and Cu^{2+} from metal plating industry effluents.

Sample	Metal ion	Eluent used	In mg/100 mL
Fertilizer industry wastewater (I)	Cd^{2+}	0.01 M NH_4NO_3	1.38
Fertilizer industry wastewater (II)	Cd^{2+}	0.01 M NH_4NO_3	1.40
Metal plating industry wastewater (I)	Cu^{2+}	0.1 M NH_4NO_3	1.75
Metal plating industry wastewater (II)	Cu^{2+}	0.1 M NH_4NO_3	1.65
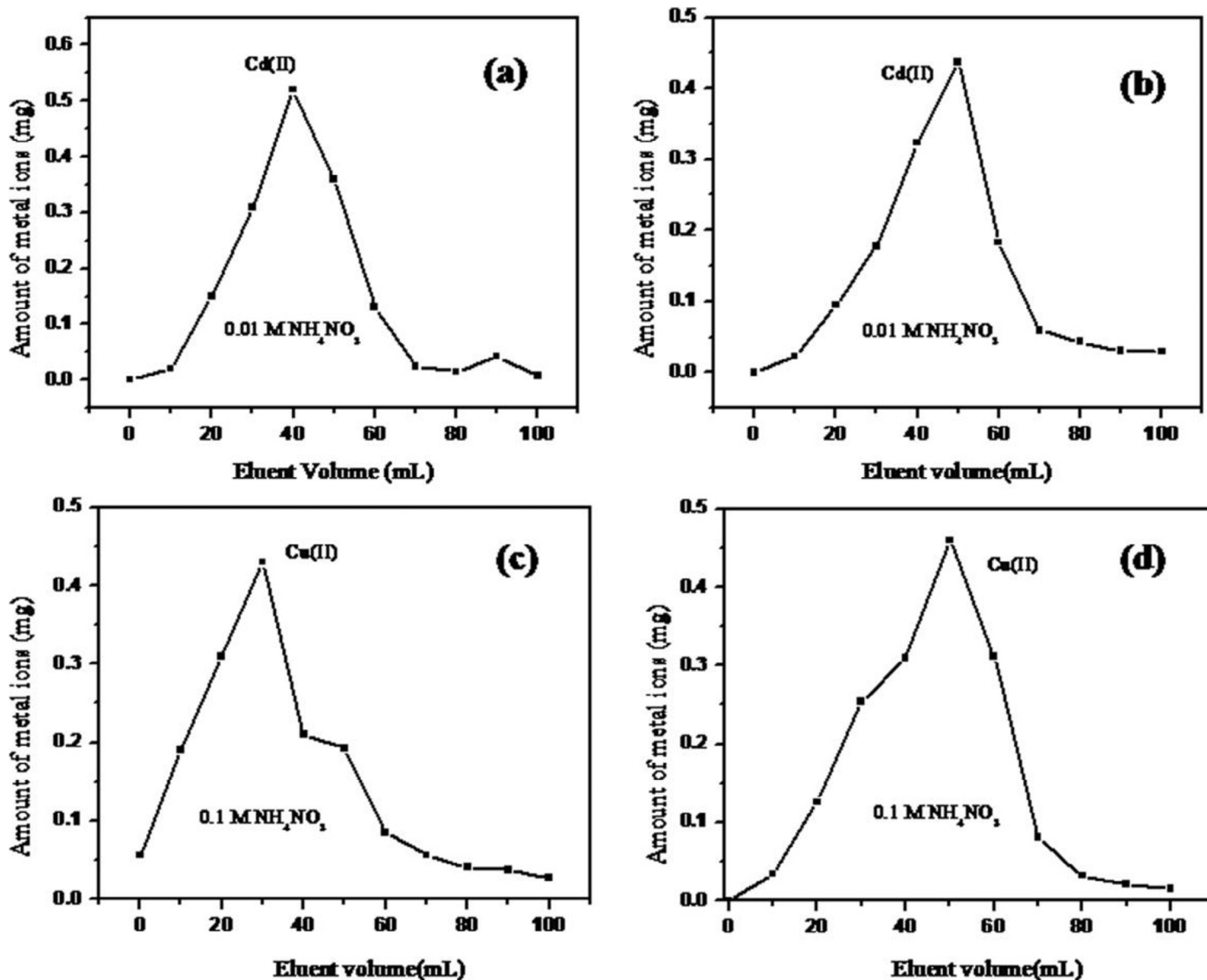
Fig. 7. Elution curves for the separation of (a and b) Cd(II) ions and (c and d) Cu(II) ions.

Pseudo-first-order (eqn. (4)):

$$\log(q_e - q_t) = \log q_e - k_1 t / 2.303 \qquad (4)$$

Pseudo-second-order (eqn. (5)):

$$\frac{t}{q_t} = \frac{1}{k_2 q_e^2} + \frac{t}{q_e} \qquad (5)$$

where q_e and q_t are the adsorption capacities at equilibrium and at time t, k_1 and k_2 are pseudo-first-order and pseudo-second-order respectively. The best fit of experimental data with predicted models was calculated by determining correlation coefficient (R^2) and error analysis was estimated by calculating normalized standard deviation (NSD) using ORIGIN software. All the kinetic parameters were calculated from linear plots (Fig. 8(a) and (b)) of pseudo-first-order and pseudo-second-order. The calculated values of k_1 and k_2 and the corresponding correlation coefficient (R^2) and NSD [27] were enlisted in

Table 5. Linear regression plot showed that experimental data give better fit and higher value of R^2 to pseudo-second-order model, compared to pseudo-first-order equation. The value of NSD calculated was low and was 1.1301 for pseudo-second-order model. These suggest that Cu (II) sorption on Pc–SnMoSi is better described by pseudo-second-order rate expressions. This proposes that the mechanism involved in the rate limiting step is chemisorption involving valence forces through sharing or exchange of electron between the adsorbent and adsorbate [28]. Similar observations were found for the sorption of Pb(II) on EDTA–zirconium(IV) iodate composite exchanger [29].

3.3.1. Mass transfer aspects of Cu(II) sorption on Pc–SnMoSi

Mass transfer aspects of sorption of Cu(II) on the exchanger were analyzed by intra-particle diffusion model suggested by Weber [30] and its linearized form was formulated as (eqn. (6))
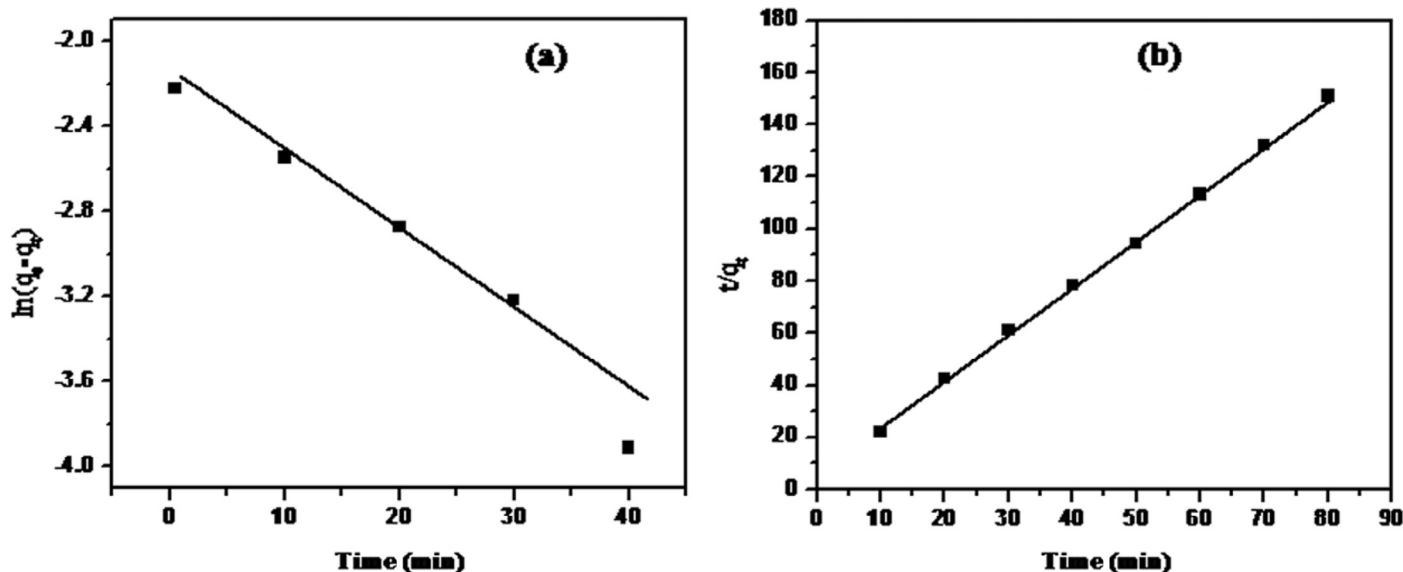
Fig. 8. Linear plots of (a) pseudo-first-order and (b) pseudo-second-order kinetic models.

$$q_t = K_d t^{1/2} + C \qquad (6)$$

where q_t is the adsorption capacities at time t, k_d is the intra-particle rate constants and C is the constant indicating thickness of the boundary layer. Linear regression plots were shown in Fig. 9. The mass transfer parameters calculated were enlisted in Table 5. It was found that the transportation of a solute into solid sorbent may be either external diffusion or film diffusion of sorbent into the external surface or intra-particle diffusion. The linear plots q_t Vs $t^{1/2}$ pass through origin suggests that intra-particle diffusion solely determine the overall rate of the reaction. Here, it can be observed that linear portion of the plots significantly deviated from origin. This deviation was due to difference in mass transfer in the initial and final stages of adsorption process. The linearity of the plots suggests that sorption of Cu(II) on Pc–SnMoSi exchanger is intra particle diffusion controlled. But deviation of regression lines from the origin indicates some extent of boundary layer control is present and that intra particle diffusion was not the only process in the rate limiting step.

3.4. Sorption isotherm

Two generally applied isotherm equations, Langmuir and Frieundlich [31], were used to model equilibrium data of sorption of Cu (II) on Pc–SnMoSi.

The linearized form of Langmuir model is given by (eqn. (7))

$$\frac{c_e}{q_e} = \frac{1}{K_L q_m} + \frac{c_e}{q_m} \qquad (7)$$

where K_L is the Langmuir constant, q_m is the maximum adsorption capacity (mg.g^{-1}) and q_e is the adsorbed amount of Cu(II) ion at equilibrium (mg.g^{-1}). The values of K_L and q_m were determined from experimental data by linear regression, i.e., a plot of c_e/q_e versus c_e (Fig. 10(a)), using ORIGINE programme (Version 6.0).

Table 5
Kinetic parameters for the adsorption of Cu^{2+} onto Pc–SnMoSi.

Pseudo-first-order			
q_e (mg/g)	K_1 (min^{-1})	R^2	NSD
0.0273	0.0412	0.9756	6.0182
Pseudo-second-order			
q_e (mg/g)	K_2 (g/mg min)	R^2	NSD
0.5524	0.05632	0.99968	1.1301
Intra-particle diffusion			
k_d	C	R^2	NSD
0.0255	0.4198	0.9856	3.3162
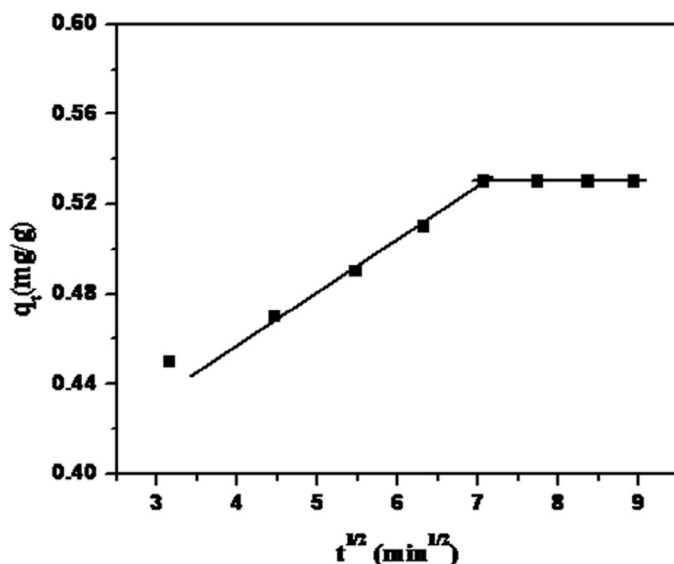
Fig. 9. Intra-particle diffusion plots of Cu(II) sorption on Pc–SnMoSi.
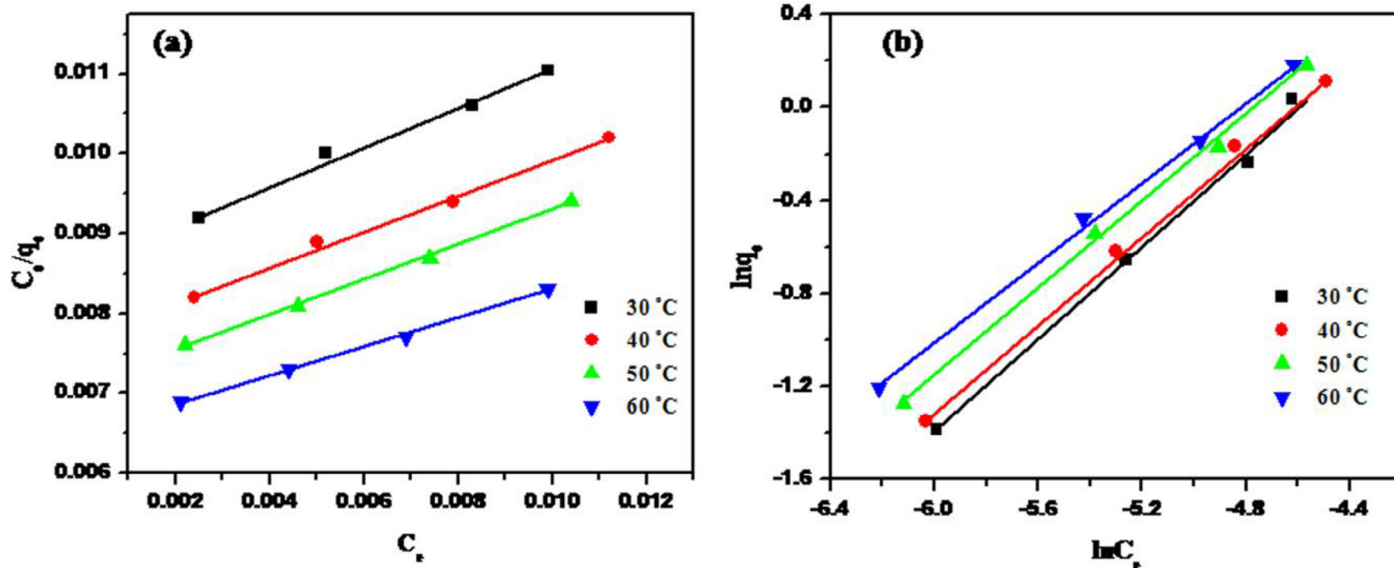
Fig. 10. Linear plots of (a) Langmuir and (b) Freundlich isotherm models.

On the other hand, the Freundlich isotherm model is expressed as (eqn. (8))

$$\ln q_e = \ln K_F + \frac{1}{n} \ln c_e \qquad (8)$$

where K_F and n are Freundlich constants related to the adsorption capacity, adsorption intensity respectively. The values of K_F and n were obtained from the linear plots of $\ln q_e$ versus $\ln Ce$ (Fig. 10(b)). Parameters calculated using linear regression analysis of both isotherms were listed in Table 6. A detailed analysis of the correlation coefficients obtained for these isotherms showed that both equations satisfactorily describe the adsorption data, but are better fitted to Langmuir than Frieundlich equation. Langmuir adsorption assumes that sorption of Cu(II) on to Pc–SnMoSi is monolayer and all adsorption sites are equivalent with uniform energies of adsorption without any interaction between the adsorbed molecules. Langmuir parameters are further used to describe the affinity between Cu(II) ions and the exchanger using the dimensionless separation factor R_L (eqn. (9)),

$$R_L = \frac{1}{1 + K_L C_e} \qquad (9)$$

The values of R_L indicate the shape of the isotherm to be either favorable $(0 < R_L < 1)$, unfavorable $(R_L > 1)$, linear $(R_L = 1)$ or irreversible $(R_L = 0)$. R_L value obtained was 0.178 suggesting favorable nature of adsorption of Cu(II) on the exchanger.

3.5. Thermodynamic properties

In order to predict the feasibility of a reaction thermodynamic study is important. All thermodynamic parameters of adsorption, i.e., enthalpy change (ΔH^0), free energy change (ΔG^0) and entropy change (ΔS^0), were calculated using the following equations (eqn. (10) and (11)) [32].

$$\Delta G = -2.303 RT \log K_L \qquad (10)$$

$$\ln K_L = \frac{-\Delta H}{RT} + \frac{\Delta S^0}{R} \qquad (11)$$

where R is the general gas constant (kJ.mol^{-1}.K^{-1}), K_L is the Langmuir adsorption constant and T is the temperature (K). ΔH^0 and ΔS^0 values can be obtained from the slope and intercept of the Van't Hoff plots of log K_L (K_L from the Langmuir isotherm) versus 1/T (Fig. 11).

The values of ΔG was −8.33, −8.73, −9.21, −9.52 kJ/mol for 30 °C, 40 °C, 50 °C and 60 °C respectively. These negative values of ΔG show the feasibility and spontaneity of Cu(II) sorption on Pc–SnMoSi composite. Positive value of ΔH (7.934kJ/mol) confirms the endothermic nature of the reaction

Table 6
Parameters for Langmuir and Freundlich isotherm models for the adsorption of Cu^{2+} ions on Pc–SnMoSi.

T (°C)	Freundlich				Langmuir			
	K_F	n	R^2	NSD	q_m (mg/g)	K_L (L/mol)	R^2	NSD
30	0.1721	0.9891	0.9823	2.2163	4.22	27.31	0.9947	1.2543
40	0.1832	1.0502	0.9867	2.3187	4.51	28.75	0.9983	1.1647
50	0.2165	1.0694	0.9917	2.0145	4.56	30.88	0.9996	1.3271
60	0.2345	1.1561	0.9721	2.4563	5.6	27.35	0.9988	1.0623
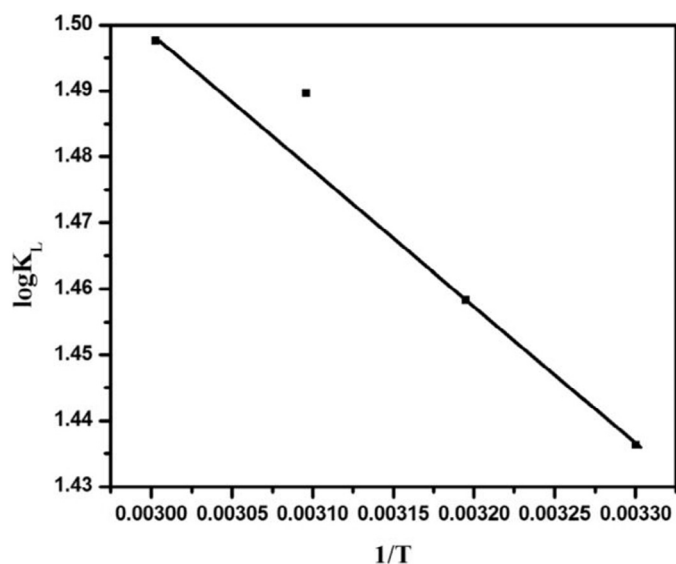
Fig. 11. Van't Hoff's plot for thermodynamic study.

which reflects the strong interaction between Pc–SnMoSi and Cu(II) ions [33]. Numerical value of ΔH predicts the ion exchange (physi sorption) behavior of the sorption process in the present study and the typical range for an ion exchange mechanism is 0–20 kJ/mol [34]. Also, positive value of ΔS^0 (7.21 J/mol/K) suggests the increased randomness during the adsorption which suggests the increased degree of freedom of coordinated water molecules.

3.6. Reusability of the exchanger

The adsorption–desorption cycles were repeated four times using 0.1 M HCl as desorbing agent and the results are shown in Fig. 12. A gradual decrease in sorption capacity of Pc–SnMoSi from 95.4 to 60.8.6% was observed after four cycles of adsorption, which may be due to loss of some amount of adsorbent in washing after every cycle. This decrease in
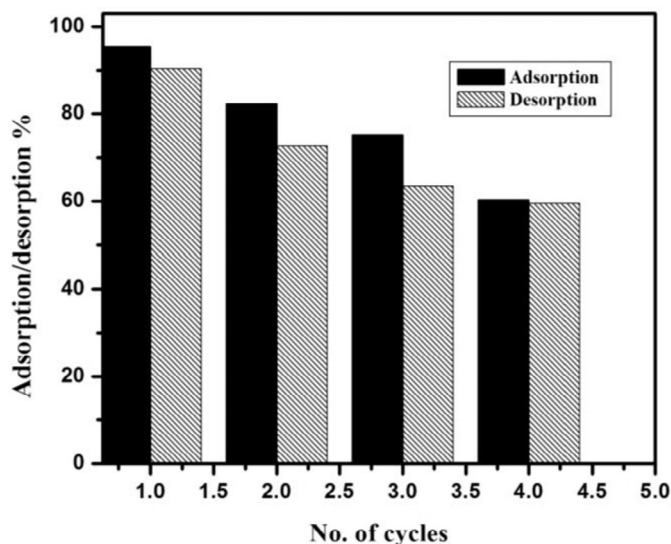
Fig. 12. Reusability test.

adsorption capacity during repeated adsorption desorption cycles validates the possibility of ion exchange interactions for Cu(II) sorption. The results in general demonstrate that Pc–SnMoSi can be used effectively for the recovery of Cu(II) and the adsorbent can be reused up to 4 cycles.

4. Conclusions

Novel biopolymer based composite ion exchanger was synthesized and well characterized. Composite formation was confirmed by comparing its physico chemical properties with its inorganic counterpart. Composite shows good ion exchange properties in comparison with the inorganic precipitate. It also shows good selectivity to toxic metal ions such as Cd(II) and Cu(II) and has been successfully separated from industrial waste water. Kinetic studies on Cu(II) sorption reveal that experimental data fit well with pseudo-second-order model. Monolayer coverage of sorption was confirmed by fitness of equilibrium data with Langmuir equation. Thermodynamic study reveals feasibility and spontaneity of sorption reaction. Desorption experiment showed that the process was repeatable and the exchanger was regenerated using 0.1 M HCl with 95% efficiency.

References

[1] J.W. Moore, S. Ramamoorthy, Monitoring and Criteria for Impact Assessment of Metals. Heavy metals in Natural Waters, 1984.

[2] S. Babel, T.A. Kurniawan, Low-cost adsorbents for heavy metals uptake from contaminated water: a review, J. Hazard. Mater. 97 (2003) 219–243.

[3] O.C.S. Al Hamouz, M.K. Estatie, M.A. Morsy, T.A. Saleh, Lead ion removal by novel highly cross-linked Mannich based polymers, J. Taiwan Inst. Chem. Eng. (2016) doi:10.1016/j.jtice.2016.10.027.

[4] G. Tiravanti, D. Petruzzelli, R. Passino, Pretreatment of tannery wastewaters by an ion exchange process for Cr (III) removal and recovery, Water Sci. Technol. 36 (1997) 197–207.

[5] G. Alberti, U. Costantino, M.L. Lucianigiovagnotti, Crystalline insoluble acid salts of tetravalent metals. 32. comparison of ion-exchange properties of crystalline alpha-titanium alpha-zirconium and phosphate, Gazz. Chim. Ital. 110 (1980) 61–67.

[6] K.G. Varshney, M.A. Khan, M. Qureshi, K.G. Varshney, Amorphous inorganic ion exchangers, Inorg. Ion Exch. Chem. Anal. (1991) 177–270.

[7] O.S. Amuda, I.A. Amoo, Coagulation/flocculation process and sludge conditioning in beverage industrial wastewater treatment, J. Hazard. Mater. 141 (2007) 778–783.

[8] B. Preetha, C. Janardanan, Kinetic studies on novel cation exchangers, antimony zirconium phosphate (SbZP) and antimony zirconium triethylammonium phosphate (SbZTP), Desalin. Water Treat. 57 (2016) 6268–6277.

[9] T.E. Agustina, H.M. Ang, V.K. Vareek, A review of synergistic effect of photocatalysis and ozonation on wastewater treatment, J. Photochem. Photobiol. C Photochem. Rev. 6 (2005) 264–273.

[10] S.E. Bailey, T.J. Olin, R.M. Bricka, D.D. Adrian, A review of potentially low-cost sorbents for heavy metals, Water Res. 33 (1999) 2469–2479.

[11] S.A. Nabi, M. Naushad, Synthesis, characterization and analytical applications of a new composite cation exchanger cellulose acetate-Zr (IV) molybdophosphate, Colloids Surf. A Physicochem. Eng. Asp. 316 (2008) 217–225.

[12] B. Lehnert, Proceedings of the Second International Conference on the Peaceful Uses of Atomic Energy, 1958.

[13] D. Pathania, G. Sharma, R. Thakur, Pectin@ zirconium (IV) silicophosphate nanocomposite ion exchanger: photo catalysis, heavy metal separation and antibacterial activity, Chem. Eng. J. 267 (2015) 235–244.

[14] A. Clearfield, Inorganic ion exchangers: a technology ripe for development, Ind. Eng. Chem. Res. 34 (1995) 2865–2872.

[15] P. Gomez-Romero, Hybrid organic – inorganic materials – in search of synergic activity, Adv. Mater. 13 (2001) 163–174.

[16] S.K. Nataraj, K.M. Hosamani, T.M. Aminabhavi, Distillery wastewater treatment by the membrane-based nanofiltration and reverse osmosis processes, Water Res. 40 (2006) 2349–2356.

[17] F.A.R. Pereira, K.S. Sousa, G.R.S. Cavalcanti, M.G. Fonseca, A.G. de Souza, A.P.M. Alves, Chitosan-montmorillonite biocomposite as an adsorbent for copper (II) cations from aqueous solutions, Int. J. Biol. Macromol. 61 (2013) 471–478.

[18] M. Naushad, Inorganic and composite ion exchange materials and their applications, Ion Exch. Lett. 2 (2009) 1–14.

[19] N. Viswanathan, S. Meenakshi, Development of chitosan supported zirconium (IV) tungstophosphate composite for fluoride removal, J. Hazard. Mater. 176 (2010) 459–465.

[20] S. Liang, X. Guo, N. Feng, Q. Tian, Isotherms, kinetics and thermodynamic studies of adsorption of Cu 2+ from aqueous solutions by Mg 2+/K+ type orange peel adsorbents, J. Hazard. Mater. 174 (2010) 756–762.

[21] R.K. Mishra, A. Anis, S. Mondal, M. Dutt, A.K. Banthia, Preparation and characterization of amidated pectin based polymer electrolyte membranes, Chin. J. Polym. Sci. 27 (2009) 639–646.

[22] O. Samuelson, Ion exchangers in analytical chemistry, 1952.

[23] G. Sharma, D. Pathania, M. Naushad, N.C. Kothiyal, Fabrication, characterization and antimicrobial activity of polyaniline Th (IV) tungstomolybdophosphate nanocomposite material: efficient removal of toxic metal ions from water, Chem. Eng. J. 251 (2014) 413–421.

[24] C.N.R. Rao, Chemical applications of infrared spectroscopy, 1963.

[25] V.K. Gupta, D. Pathania, P. Singh, Pectin – cerium (IV) tungstate nanocomposite and its adsorptional activity for removal of methylene blue dye, Int. J. Environ. Sci. Technol. (Tehran) 11 (2014) 2015–2024.

[26] C. Raji, T.S. Anirudhan, Batch Cr (VI) removal by polyacrylamide-grafted sawdust: kinetics and thermodynamics, Water Res. 32 (1998) 3772–3780.

[27] M.G. Pillai, P. Simha, A. Gugalia, Recovering urea from human urine by bio-sorption onto microwave activated carbonized coconut shells: equilibrium, kinetics, optimization and field studies, J. Environ. Chem. Eng. 2 (2014) 46–55.

[28] K.G. Bhattacharyya, A. Sharma, Kinetics and thermodynamics of methylene blue adsorption on neem (Azadirachta indica) leaf powder, Dye. Pigment. 65 (2005) 51–59.

[29] M. Naushad, Z.A. ALOthman, H. Javadian, Removal of Pb (II) from aqueous solution using ethylene diamine tetra acetic acid-Zr (IV) iodate composite cation exchanger: kinetics, isotherms and thermodynamic studies, J. Ind. Eng. Chem. 25 (2015) 35–41.

[30] P. Simha, A. Yadav, D. Pinjari, A.B. Pandit, On the behaviour, mechanistic modelling and interaction of biochar and crop fertilizers in aqueous solutions, Resour. Efficient Technol. 2 (2016) 133–142.

[31] J. De Los Santos, J.M. Cornejo-Bravo, E. Castillo, N. Bogdanchikova, S.M. Farias, J.D. Mota-Morales, et al., Elimination of sulfates from wastewaters by natural aluminosilicate modified with uric acid, Resour. Efficient Technol. 1 (2015) 98–105.

[32] D. Mohan, K.P. Singh, Single-and multi-component adsorption of cadmium and zinc using activated carbon derived from bagasse – an agricultural waste, Water Res. 36 (2002) 2304–2318.

[33] T.S. Anirudhan, P.S. Suchithra, P. Senan, A.R. Tharun, Kinetic and equilibrium profiles of adsorptive recovery of thorium (IV) from aqueous solutions using poly (methacrylic acid) grafted cellulose/bentonite superabsorbent composite, Ind. Eng. Chem. Res. 51 (2012) 4825–4836.

[34] Y. Yu, Y.-Y. Zhuang, Z.-H. Wang, Adsorption of water-soluble dye onto functionalized resin, J. Colloid Interface Sci. 242 (2001) 288–293.